Shahrood University of Technology

Journal of Mining and Environment (JME)

Journal homepage: www.jme.shahroodut.ac.ir

Iranian Society of Mining Engineering (IRSME)

Experimental Investigation on Self-closure Mechanism of Mudstone Fractures and Permeability Variation of Mining Overburden

Weiqun Liu, Tian Fang*, and Sheng Sang

State Key Laboratory for Geomechanics and Deep Underground Engineering, China University of Mining and Technology, Xu Zhou 221116, Jiangsu

Article Info

Received 3 November 2024

Received in Revised form 1 December 2024

Accepted 14 January 2024

Published online 14 January 2024

DOI: 10.22044/jme.2025.15302.2935

Keywords

Fracture closure

Mudstone

Viscoelasticity

Strain softening behavior

Soil water

Abstract

Mudstone is a common rock in underground engineering, and mudstone with fractures, have the certain self-closing capability. In this paper, we employed experiments and numerical analyses to investigate the mechanism of such a characteristic, and also examined the permeability pattern of mudstone overburdens. The experiments were performed with the MTS815.02 testing system, involving material properties under different water contents and their crack-closing behaviors. The principal task of numerical analysis is to determine the permeability of fractured mudstone layers, working with the COMSOL platform. The experimental results show that the Young's Modulus of water-saturated mudstone is just 2.2% of that of natural mudstone, and the saturated also exhibit a remarkably obvious creep behavior. As the surrounding pressures increase, the permeability coefficient of fractured mudstone decrease exponentially, even dropping by two orders of magnitude corresponding to over 2.0MPa pressures. Based on these experiment outcomes, we can easily infer that rapid or complete fracture-closing is the main reason of permeability drop, and furthermore, both softening and creep are the major factors of self-closure of mudstone fractures, and especially, the softening behavior plays an absolutely fundamental role. The numerical analyses show that either a higher in-situ stress or lower fracture density can obviously become one of the advantageous conditions for fractured mudstone layers to restore towards impermeability. These results are also verified by the engineering observation in Yili No. 4 mine of China. There obviously existed the recovery of water-blocking capacity of overlying strata after a period of time. We hereby recommend this investigation as refences for underground mining or engineering construction involving mudstone.

1. Introduction

Vegetation is an important indicator of the ecosystem in the area and the most intuitive reflection of the natural environment. Vegetation grows in the soil, and most of the water needed comes from the soil. There is a strong correlation between groundwater level, soil water content, and vegetation diversity. Generally, the coal seams with mining value are located below the underground aquifer. According to the supply and loss paths of soil water, the factors affecting soil water are divided into the recharge and leakage in rock layers, radial flow of the soil layer, atmospheric precipitation, and evaporation (including vegetation transpiration). After mining, as shown in Figure 1, a large amount of soil water lost along the through fractures in the rock formations, which seriously disrupted the supply and demand balance of soil water. Consequently, the original vegetation probably withers gradually after mining.

As shown in Figure 2, northwestern China is far from the sea, and surrounded by mountains and plateaus, which makes the amount of precipitation in the region less and unevenly distributed. The vegetation is more dependent on soil water in the arid and semi-arid regions of northwest China, compared with that in the areas with abundant rainfall. Therefore, coal mining and environmental carrying capacity in northwestern China are the

Corresponding author: 357421666@qq.com (T. Fang)

contradictions that plague China's regional economic and social development.

Combined with the geological data of the Northwest coal mining area, most of the overlying strata contain mudstone, and mudstone strata are regarded as the main water barrier. After the coal seam is excavated, the overburden rock layer including mudstone is disturbed to form fractures, and thereby, the overburden rock layer has no water retention capacity. The natural moisture content of mudstone is between 3 and 5%, which is a state of low moisture content. After soil water entered the fracture, the water immersed into the mudstone matrix in a direction perpendicular to the wall surface of the fracture, so that the moisture content of the matrix surrounding the fracture become saturated. However, after the mudstone encounters water, the mechanical properties of the mudstone also change with the increase of saturation [1-4]. When certain conditions and time are met, the mudstone layer also has a certain recovery of water blocking.

To systematically investigate the water-blocking mechanism of mudstone overburdens, Yili No. 4 Mine in Yili City, Xinjiang, China are selected as an field background. Yili No. 4 Mine is located in the southeast of Huocheng County, Yili City, Xinjiang, China. Its geological structure and topography is shown in Figure 2.

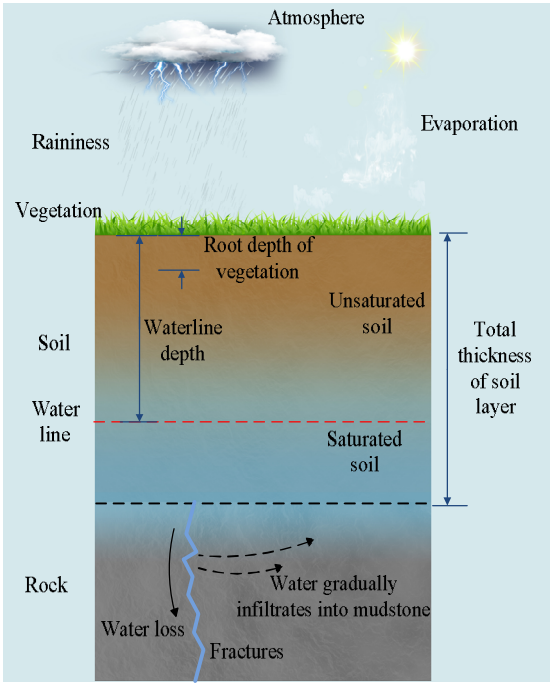

Figure 1. Schematic diagram of soil water leakage.

Order number	Tthickness /m	Histogram	Character
1	18.0		Soil
2	12.0		Conglomerate
3	24.0		Mudstone
4	18.0		Coarse sandstone
5	6.0		Argillaceous siltstone
6	4.6		Mudstone
7	8.0		Coarse sandstone
8	8.0		Sandstone
9	11.0		Mudstone
10	8.0		Sandstone
11	6.4		Mudstone
12	12.0		Siltstone
13	8.0		Mudstone
14	6.0		Coal 21-1
15	10.0		Mudstone

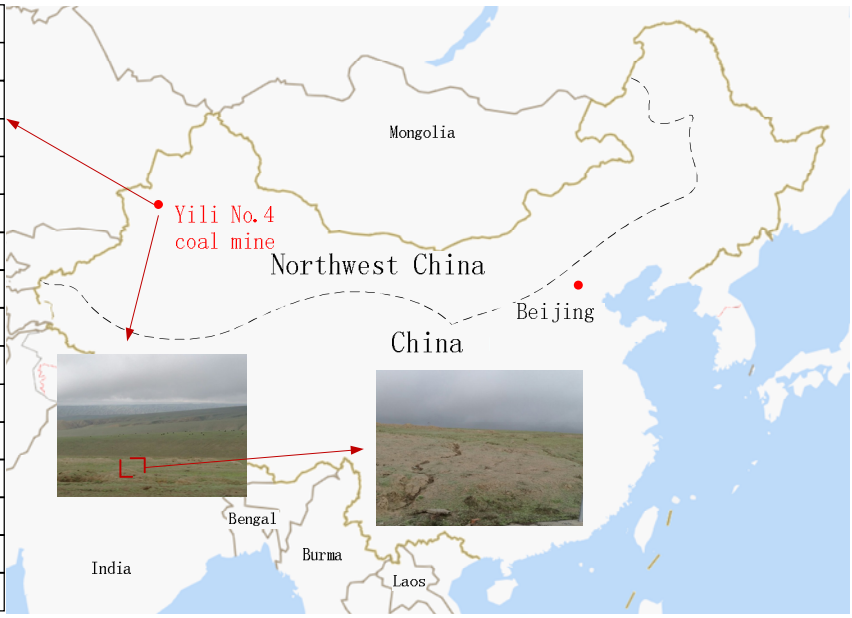

Figure 2. Stratigraphic structure and topography of the No. 4 Yili Mine.

The coal field is a low-mountain hilly landform, with an overall topography of northeast high and southwest low. The Yili Basin is a Mesozoic mountain depression basin. The sedimentary bases are Permian, Carboniferous, and Devonian strata of the Upper Paleozoic. The Upper Paleozoic strata are distributed in the mountains surrounding the basin, and the Quaternary and Neogene strata are widely distributed on the surface of the basin. Jurassic and Triassic strata are exposed from the mountain to hilly areas at the edge of the basin. Jurassic strata are dominated by sandstone,

mudstone and coal. Among them, mudstone layers and a coal layer are the main water barriers, and sandstone layers and an intercalated conglomerate layer are weak aquifers. The rock condition from the surface to the main coal seam (21-1) is shown in Figure 2. The upper and lower weak aquifers composed of loose pebbles and coarse sandstone are recharged by precipitation, and the dynamics of shallow water are significantly affected by seasonal changes.

In addition to soil water loss caused by mining [5, 6], in most underground rock engineering such as nuclear waste storage and oil & gas exploitation fractures are important seepage channels [7-11]. With the passage of time, new fractures are formed around the rock mass, in which, the project is located. In special working conditions, especially nuclear waste storage and soil water loss caused by mining, the rock permeability should be consistently maintained at a low level. Soft rocks with self-closing fractures will have an important role[12]. Mudstone, a soft rock, is widely distributed in strata [13, 14]. Mudstone fractures have a self-closing capability under certain conditions [1, 7]. Therefore, an investigation of the self-closing characteristics of mudstone fractures has significance.

Research on the self-closing behaviors of fractures can be divided into physical and chemical effects according to the closure mechanism. Chemical effects are mainly caused by the decomposition and recombination of chemical constituents in rocks such as the transfer of calcium carbonate through water flow [15-19]. According to chemical reaction characteristics, Brunet JPL et al. obtained the conditions for the self-closure of a cement fracture such as the fracture width and flow rate [19]. It takes a long time and specific conditions for chemical effects to cause fractures closure. Physical effects include the blocking of fractures by particles in fluids [16], and weakening of the mechanical properties of the matrix around the fracture to reduce its aperture [20, 21]. X-ray imaging and surface analysis show that the largest alteration due to cement dissolution occurred near to the inlet, where the injected brine was the most reactive, while precipitation occurred in the middle section and negligible change occurred in the outlet section [16]. It is a complex and accidental process for particles in fluid to block fractures, so we will not study it in detail. Currently, an investigation of the physical properties of the rocks around fractures focuses on rock expansion and rock damage [1, 13, 20]. However, rock expansion and rock damage can not accurately reflect the self-closing of fractures.

In this paper, the influence of the mudstone properties on fracture closure is analyzed by means of experiments. The mudstone samples of the Baoli open-pit coal mine in Erdos city, Inner Mongolia, China, is applied as the research object. The mudstones of Baoli open-pit coal mine have the same composition and properties as those of Yili No. 4 Mine. The conditions of the experiment were changed and compared with the experimental results to obtain all factors that affect the fracture self-closing. According to the investigation of the fracture self-closing factors in this paper, the capability of fracture self-closing can be estimated by use of conventional mechanical and creep tests on mudstone samples. The self-closing of mudstone fractures can attribute to the reduction of the initial normal stiffness of the fractures. Based on the experimental data, the permeability changes of fractured mudstone layers under different fracture densities and stress conditions are analyzed with the COMSOL platform. Combined with the geological structure and stress conditions of the Yili No. 4 Mine, the permeability of the mudstone layer is estimated, which provides a corresponding reference for the production and post-production maintenance of the mine. In addition, this research can provide important references for related fields with underground rock seepage problems.

2. Mudstone Specimens

We prepared mudstone samples with a natural water content from 2.8~3.8% and a saturated water content from 11.0~17.9%. After soaked in water, the samples are easily saturated through a relatively short time, even though some of the samples have more or less damage. The experiments show that for the samples with different saturations, over 11% the mechanical characteristics are extremely similar. As a result, our saturating procedure is that no sooner do the contents reach 11% than we pick up the samples from water to prepare next steps. In this experiment, the MTS815.02 electrohydraulic servo-controlled rock mechanics testing system was used to analyze the rock mechanics, as shown in Figure 3. The uniaxial compression test was adopted, and the loading speed was 0.05 mm/min. The elastic modulus of natural mudstone is 2.78 GPa, while that of saturated mudstone is 0.06 GPa. These basic mechanical parameters are listed in Table 1. In addition, we also tested that the

expansion rate of mudstone is 0.015.

The MTS815.02 testing system is also used in the uniaxial creep testing of the specimens. The loading stress is approximately 30% of the uniaxial compressive strength of the mudstone, and the creep time is approximately 1 hour.

The viscous deformation of rock is shown in Figure 4. The viscous deformation of the mudstone with a low water content is very small, while the viscous deformation of the saturated mudstone in one hour exceeds its elastic deformation. Therefore, saturated mudstone exhibits a notable viscoelastic behavior.

Table 1. Basic mechanical parameters of the mudstone, as obtained by experiments.

Rock	Water content of the mudstone	Young's modulus (GPa)	Poisson's ratio	Uniaxial strength (MPa)
Mudstone	Natural (3~5%)	2.78	0.23	11.6
	7%	0.67	0.45	2.2
	Saturated	0.06	0.39	0.7

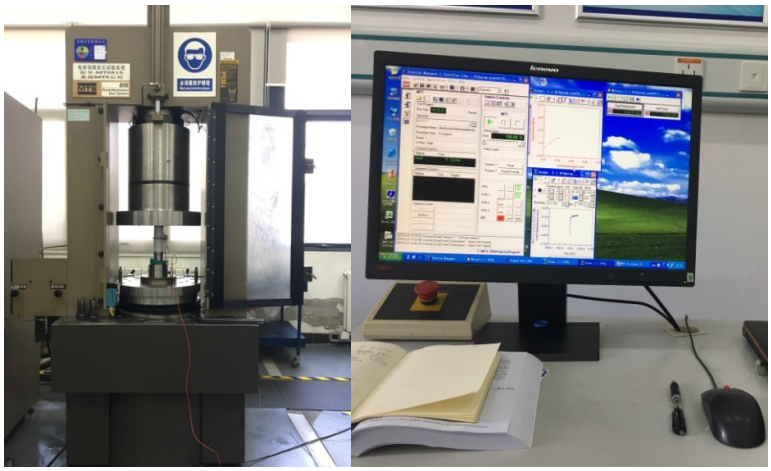

Figure 3. MTS815.02 Electrohydraulic Servo-controlled Rock Mechanics Testing System.

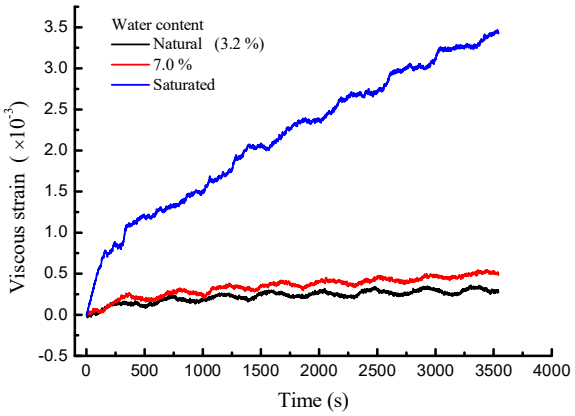

Figure 4. Viscous strain curves of mudstone with different water contents.

As shown in Figure 5, we use a method similar to Brazilian splitting to produce a single fracture through the specimen. The mass loss of the specimens in the process of fracturing is very small. Except for the main fractures, nearly no new fractures are formed in the rock matrix. With this approach, the success rate of samples preparation is higher than 70% despite of the weak consolidation of mudstone.

Since the fractured samples are machine-fabricated from natural intact rocks, the cracks can occupy certain coarseness, so are more similar to the reality. The asperities and depressions along the two fracture walls are coupled with each other. As a result, the contact area of the fractures is large, but the actual hydraulic aperture of the fractures is very small. To highlight the experimental phenomena, the two half parts of the fractured specimen are separated along the axial direction. As shown in Figure 5, the separated specimen is wrapped with PVC tapes to prevent the sides of the specimen from adhering to the rubber cylinder in the rock sample holder.

3 Seepage Experimental System considering Fracture Closure

In this paper, the closure process of mudstone fractures in the seepage process is examined and measured by experiments. Therefore, the experimental equipment needs to have the function to perform long-term and stable measurements. In addition, the equipment should have a large

metering range, which can span 4-5 orders of magnitude. The traditional equipment has certain shortcomings in completing the experiment. According to the needs of the experiment, an experimental system of fracture seepage considering fracture opening and closure is developed. The system can be used for both water permeation and gas permeation experiments. Its schematic diagram is shown in Figure 6.

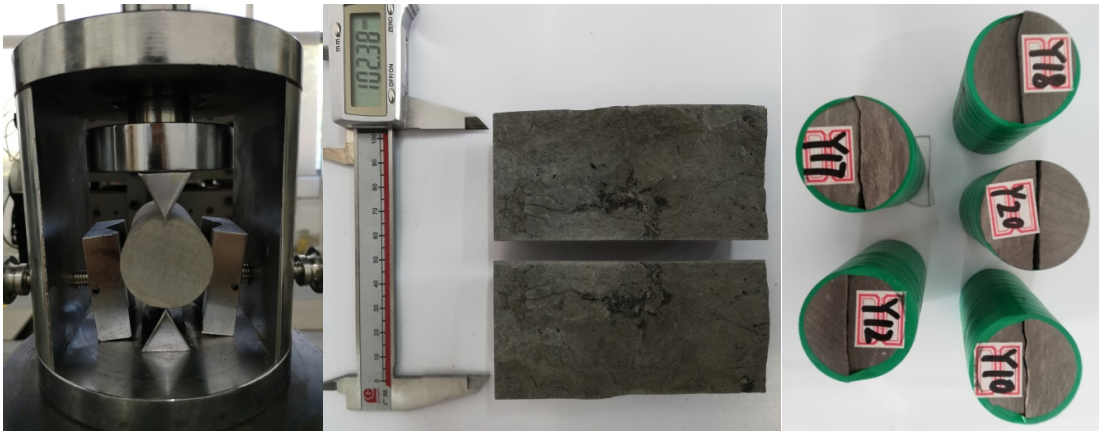

Figure 5. Single-fracture mudstone samples prepared by Brazilian splitting.

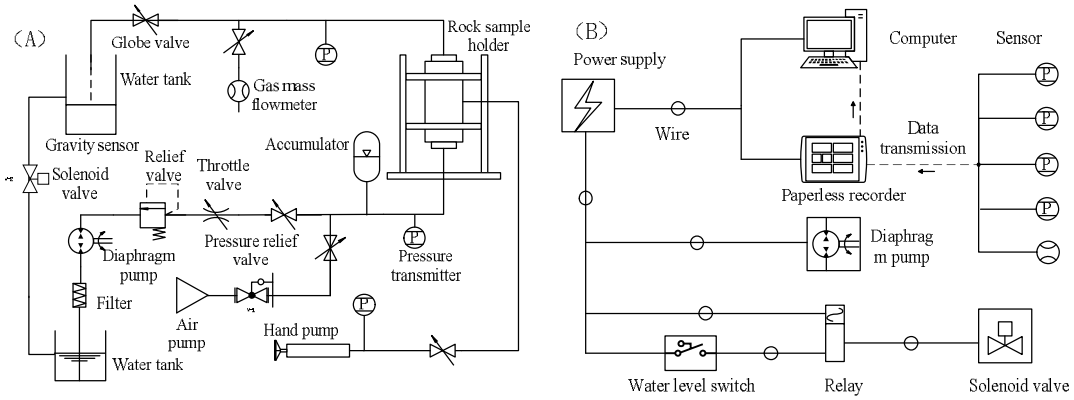

Figure 6. The principal diagram of experimental system of fracture seepage.

Because the regular meters occupy small measurement ranges, usually spanning two orders of magnitude, the experimental requirements cannot be satisfied. Therefore, we employed gravity sensors to measure the cumulative mass of water passing through the fractures, and then calculates the speed of gravity variation. To ensure the uninterrupted operation of the gravity sensors, when the liquid in a tank above the gravity sensors reaches a certain water level, a relay-controlled solenoid valve is opened, and the solenoid valve is closed after all the water is discharged from the tank. The accuracy of flow measurement by this method depends on the accuracy of the gravity sensor and sampling interval. Through inspected beforehand, the system can meet the experimental requirements for measurement accuracy.

There is a pipeline between the upstream and downstream pressure transmitters of the rock sample holder, apart from the fractures in the rock sample. When water passes through the pipeline, a pressure loss will occur. It is the pressure loss of the experimental system, which should be removed when the experimental data are processed. By testing the pressure loss of the system at different flow rates, we drew the pressure loss curve of the system, as shown in Figure 7. The pressure loss equation of the water passing through the experimental system, which was obtained by fitting the measured data, is as follows:

$$p_{sw} = 20.8Q_w^{\ 2} \quad (1)$$

where, the fitting degree is $R^2 = 0.999$, p_{sw} is the pressure loss of the water flowing through the experimental system, kPa, and Q_w is the water flow, L/min. Due to different permeable media, the pressure loss curves of the system also differ. The

pressure loss of the gas passing through the experimental system is defined as:

$$p_{sg} = 0.0318 Q_g^2 \quad (2)$$

where, the fitting degree is $R^2 = 0.998$, p_{sg} is the pressure loss of the gas flowing through the experimental system, and kPa, and Q_g is the gas flow rate, L/min.

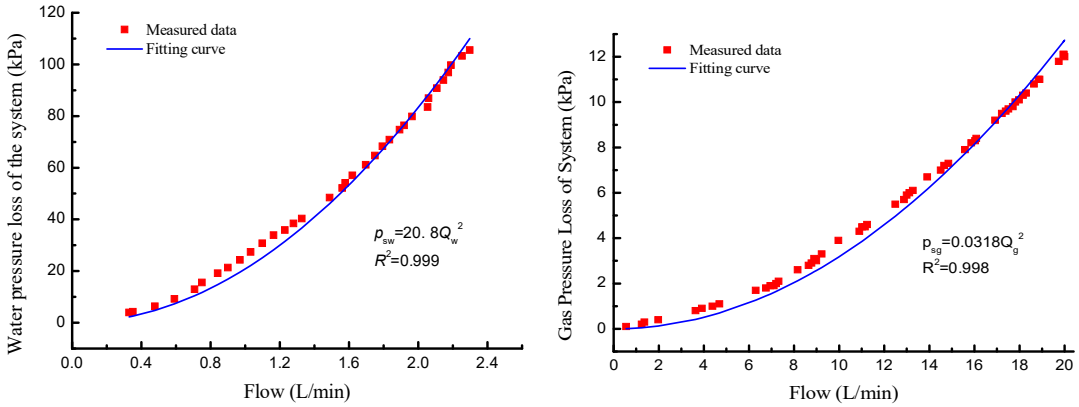

Figure 7. Water and gas pressure loss curves of experimental system.

The experimental system is continuously debugged and tested within 15 days. In the whole measurement process, the pressure and flow rate are stable, so are the data collecting and recording systems. This observation shows that the experimental system has a continuous working capability and satisfies the experimental needs.

4. Fracture Closure Experiments of Mudstone with a Natural Water Content

The mudstone matrix has a very low permeability coefficient of 3.13 × 10-10 m/s, usually being regarded impermeable. In other words, with the fixed confining pressure and different osmotic pressure differences, the permeability coefficient of the same mudstone sample remains constant; thus, we proposed that fracture seepage can be described by Darcy's law [22]. This paper mainly examines and analyzes the permeability coefficient of the rock samples and hydraulic opening of the fractures [21].

$$K = -\frac{Q}{AJ} = -\frac{QL'\rho g}{A(\Delta p - p_s)} \quad (3)$$

Where, K is the permeability coefficient, A is the cross-sectional area of the sample, L' is the length of the sample, Q is the flow flux through the sample, ρ is the density of the fluid medium, g is the gravitational acceleration, Δp is the difference between the upstream pressure and downstream pressure, and p_s is the pressure loss of the system.

According to the geometrical shape of the fracture through the sample, the length of the fracture L in the experiment is the length of the sample L' minus the displacement of the shear distance, and the width of the fracture is the diameter of the sample w. The hydraulic opening of the fracture is defined as:

$$b_h = \sqrt[3]{-\frac{12\mu QL}{w(\Delta p - p_s)}} \quad (4)$$

where, b_h is the hydraulic opening of the rough fracture, and μ is the dynamic viscosity coefficient of the fluid medium. With regards to water only, when the permeability coefficient is smaller than 5.00 × 10^{-9} m/s, the sample is an actually impervious material. This permeability can be converted to the hydraulic opening 6.27 × 10^{-6} m. The hydraulic opening of fractured mudstone is smaller than 6.27 × 10^{-6} m, and furthermore its real hydraulic opening is almost 0.0 m.

First, the fractured mudstone samples with a natural water content is placed into the rock sample holder. The confining pressures were set to 0.5 MPa, 1.0 MPa, 1.5 MPa, 2.0 MPa, and 2.5 MPa, and each confining pressure remained unchanged during an experimental period. The permeability pressure differences were set to 0.16 MPa and 0.35 MPa, and each permeability pressure difference remained unchanged during an experimental period, too. The permeability coefficients of the

fractured mudstone samples were continuously tested, and the test time is 72 hours. At the end of the test, the sample is completely saturated. The experiment duration is short, and pure water is used as the permeating medium. Therefore, there were almost no chemical effects in the fracture closure experiment.

The permeability and hydraulic opening of each sample at the beginning and end of the experiment are listed in Table 2. The hydraulic opening of the fractures in the Y3, Y8, Y16, Y17, and Y22 samples substantially varies, with all changes greater than 6.50 × 10-5 m. At the end of the experiment, the hydraulic opening of samples Y1, Y16 and Y18 is near 6.27 × 10-6 m, and the fractures approach complete closure. The permeability coefficient of all specimens in this part decreases by 75~100%, and the corresponding hydraulic opening of the fractures decreases by 37~100%.

Table 2. Permeability of the samples and fracture hydraulic opening before and after the experiments.

Sample	Confining pressure (MPa)	Osmotic pressure difference (MPa)	Permeability coefficient of the sample			Hydraulic opening of the fractures		
			Initial time (m/s)	End time (m/s)	Proportion reduction (%)	Initial time (m)	End time (m)	Proportion reduction (%)
Y12	0.500		1.02×10^{-5}	2.56×10^{-6}	74.9	7.95×10^{-5}	5.01×10^{-5}	36.9
Y16	1.00		5.49×10^{-5}	5.91×10^{-8}	99.9	1.39×10^{-4}	1.43×10^{-5}	89.8
Y18	1.50	0.160	5.35×10^{-6}	7.90×10^{-8}	98.5	6.41×10^{-5}	1.57×10^{-5}	75.5
Y8	2.00		6.35×10^{-6}	0.00	100	6.79×10^{-5}	0.00	100
Y17	2.50		5.89×10^{-6}	0.00	100	6.62×10^{-5}	0.00	100
Y22	0.500		6.07×10^{-5}	4.18×10^{-6}	93.1	1.44×10^{-4}	5.90×10^{-5}	59.0
Y3	1.00		6.89×10^{-5}	1.44×10^{-6}	97.9	1.50×10^{-4}	4.14×10^{-5}	72.5
Y15	1.50	0.350	9.88×10^{-6}	2.82×10^{-7}	97.1	7.86×10^{-5}	2.40×10^{-5}	69.4
Y1	2.00		8.41×10^{-6}		99.0	7.45×10^{-5}	1.60×10^{-5}	78.5
Y7	2.50		3.01×10^{-6}	0.00	100	5.29×10^{-5}	0.00	100

Because the roughness of the fracture in each specimen differs, its variation curve for each specimen is unique [23]. The experimental results showed that the influence of the osmotic pressure difference on the fracture closure is very small, while the normal stress of the fracture has a significant promoting effect on the fracture closure. When the confining pressure reaches 2.0~2.5 MPa, the permeability coefficient of the specimen Y7, Y8 and Y17 rapidly decreases until the permeability coefficient is smaller than 5.0 × 10-9 m/s. The fractures in these samples are completely closed, and the permeability decreases by three orders of magnitude. Sample Y8 completed the process in 105 minutes and sample Y17 in 174 minutes. The hydraulic opening of the fracture in sample Y7 is initially 5.29 ×10-5 m, but its fracture is completely closed after 68 minutes.

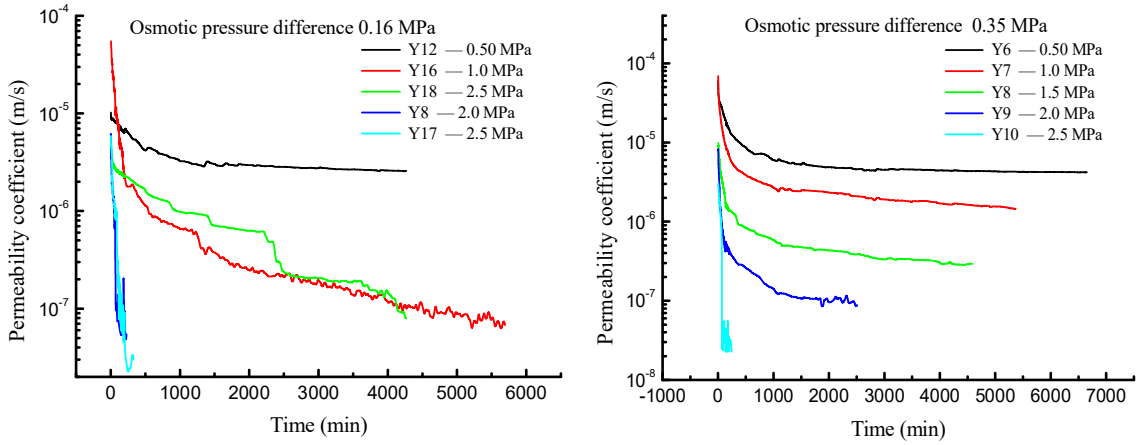

Figure 8. Variation curves of the permeability of the fractured mudstone samples at different osmotic pressures and confining pressures.

The permeability coefficient variation curves of the fractured specimens decrease exponentially with time, as shown in Figure 8. In the initial stage of the experiment, the permeability coefficient of the rock decreases rapidly. The higher the confining pressure is, the faster the permeability coefficient decreases. In the middle and final stages of the experiment, with an increase in the

experimental time, the mudstone around the fracture gradually becomes saturated. As a results, the mudstone matrix becomes soft and viscous; the stress on the contact area of the fracture decreases; the contact area of the fracture increases; the hydraulic opening of the fracture decreases; and the permeability coefficient of the sample decreases slowly.

Accordingly, the fracture hydraulic opening also changes exponentially, as shown in Figure 9. The hydraulic opening is reduced by an order of magnitude during the experiment. At the end of the experiment, the higher the confining pressure is, the smaller the hydraulic opening of the fracture is. However, the closing velocity of the fracture does not have a direct relation with the normal stress of the fracture. Probably, it is related to the roughness of the fracture.

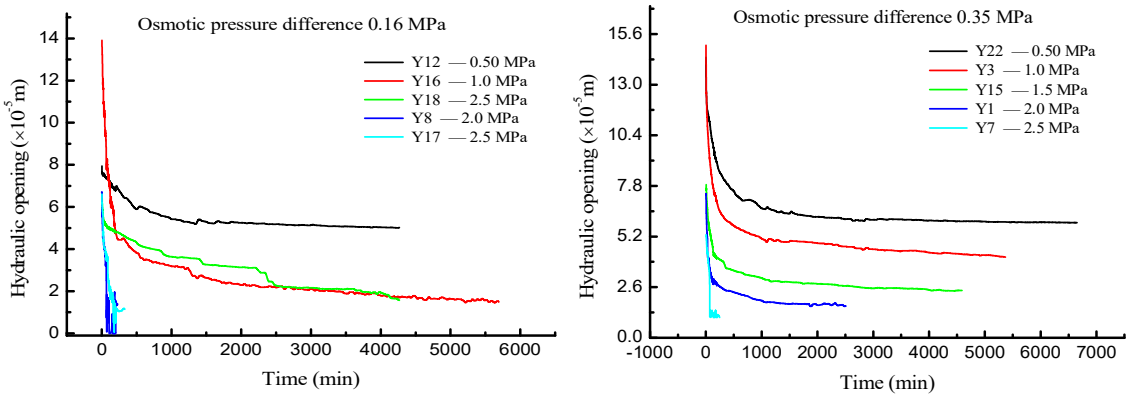

Figure 9. Hydraulic openings of the mudstone fractures at different osmotic pressures and confining pressures.

5. Analysis of Fracture Closure Factors

At the beginning of the experiments in the previous section, the fractures are dry, and the matrix around the fracture wall is unsaturated rock, so the fracture asperities can withstand a high stress. Meanwhile, the hydraulic opening of the fracture is large at the initial time, and also the permeability coefficient of the specimen is high.

In the initial stage of the experiments, a large number of mudstone particles were carried out of the test system by the water flow and deposited in the buckets. Thus, it can be inferred that the hydraulic denudation of fracture walls mainly occurred in this stage. As water enters the fracture deeper, the rock grains that are easily detached from the fracture wall are gradually removed with water flow. Simultaneously, the mudstone absorbs water and becomes gradually saturated, and the mechanical properties of the mudstone around the fracture have been weaken gradually. In the process of seepage, the elastic modulus of the mudstone decreases and the viscosity increases, and a large number of mudstone particles are denuded from the fracture wall.

For a comparison, we used air as the flowing liquid to examine fracture closure. The aerodynamic openings of samples with the natural water content are shown in Figure 10. The aerodynamic opening of the sample remains constant, like the initial value, and the permeability coefficient of the fractured mudstone remains relatively large.

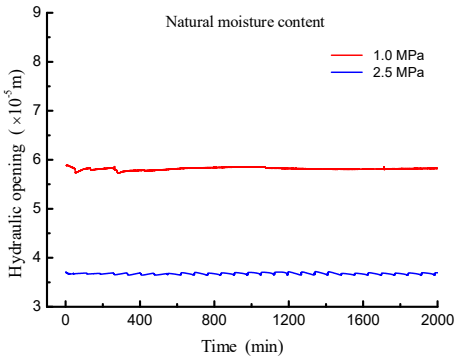

Figure 10. Aerodynamic opening of fractured mudstone with natural moisture content at different confining pressures.

The experimental observation shows that almost no mudstone particles have been eroded by air. The water content of the natural mudstone samples remains unchanged during the permeation process, and thereby, the elastic modulus of the mudstone remains nearly unchanged, while also the rheology of the mudstone remains insignificant. Compared with the experiments in the previous section, the causes of mudstone fracture closure, can be summarized as follows: hydraulic

denudation of fracture walls, softening behavior of water-soaked mudstone, and creep behavior. Meanwhile, although such three factors promote fracture closure, the effect of each factor cannot be obtained from the experiment in the previous section. In this section, the effects of different factors were investigated corresponding to the variations of the water contents and fluid media.

The hydraulic denudation of the fracture walls of mudstone can be reflected in the height loss of the support asperities between the two walls. Generally, the larger the number of particles that are denuded, the more notable the denudation effect is. To minimize the erosion of mudstone fracture wall, caused by water scouring, the condition of the equal time interval measurement is established, and a periodic water permeability test were performed. The test time is only 2 minutes each time, and the permeability pressure difference is 0.08 MPa. The test is conducted 20 times a day, and no water pressure exists in the fracture beyond the test time. Only a very small amount of mudstone particles was washed out of the experimental system. In this case, the variation curves of the permeability coefficients are shown in Figure 11.

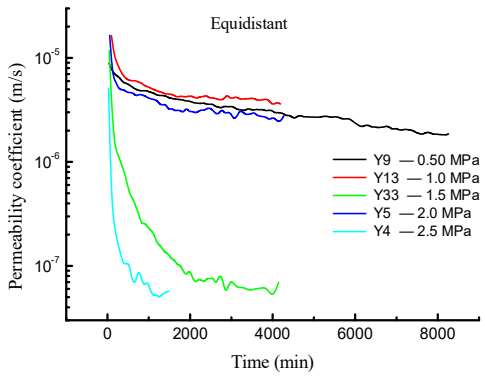

Figure 11. Permeability coefficients of fractured mudstone obtained by the equal-time-interval measurement

As shown in Figure 11, the variation curves are very similar to those shown in Figure 9. The difference is that the change rate of the permeability coefficient of each sample is lower than that shown in Figure 9. The permeability coefficients of Y4 and Y5 decrease by three orders of magnitude when the confining pressure reaches 2.0~2.5 MPa; the permeability coefficient of Y4 is smaller than 5.0 × 10-9 m/s after 20 hours of the experiment; and the fracture is completely closed. Compared with the experimental condition of a constant pressure difference, the closure time of Y4 is 8~15 times longer. The attenuation of the permeability coefficient of the other samples at a confining pressure of 0.50~1.50 MPa is only one order of magnitude. Compared with the experiment with a constant pressure difference, the change speed of the initial stage is lower, but at the end of the experiment, the hydraulic opening of the fracture decreases notably. The hydraulic denudation of fractures is very slight in this group of experiments, but the regularity process of mudstone fracture closure is consistent with that during the experiments described in the previous section. Therefore, we propose that hydraulic denudation has little effect on mudstone fracture closure.

Secondly, we analyze the effects of mudstone softening and strong viscoelasticity on fracture closure. Mudstone softening mainly refers to the decrease in elastic modulus and the increase in Poisson's ratio of the mudstone. Usually, the elastic modulus of mudstone refers to the instantaneous deformation capability of mudstone, while viscoelasticity refers to the deformation capability of mudstone with time. The stronger the viscoelasticity is, the stronger the deformation capability of the mudstone with time. The viscoelasticity of mudstone can usually be expressed by the time function of the elastic modulus. In the literature [24-27]; the closure of a fracture is the relative displacement of the fracture walls. The displacement of the fracture asperities is related to the matrix of the rock.

$$\overline{\delta} = m\frac{P(1-v^2)}{E\sqrt{A}} \tag{5}$$

where, P is the totally applied load, v is Poisson's ratio, E is Young's modulus, A is the loaded area, and m is a constant that depends on the geometry of the loaded area.

If the fracture geometry has been determined, the smaller the modulus of elasticity is, the more notable the fracture closure is. Therefore, the fracture opening of fractured mudstone is notably closed after saturation. According to the elastic modulus change with time, the process of fracture closure can be divided into instantaneous closure and gradual closure with time.

With the gradual saturation of the mudstone matrix in the experiments in the previous section, the viscoelastic deformation of mudstone matrix increases. We saturated the fractured mudstone samples with water, and then loaded the samples into the sample holder. The confining pressure is 1.0 MPa and 2.5 MPa. To keep the moisture content of the sample unchanged during the experiment,

the method of equal-time-interval gas permeation testing is also used in this part of the experiment. The variation curve of the permeability coefficient is shown in Figure 12.

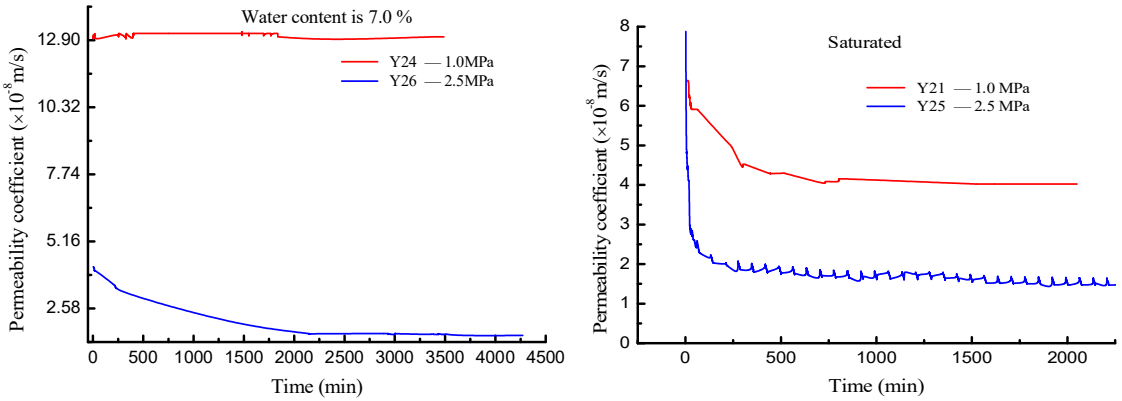

Figure 12. Gas permeability coefficients of the saturated mudstone samples at different water contents corresponding to different confining pressures.

In this part of the experiment, only a few mudstone particles are carried out of the experimental system by the flowing air, so the denudation effect of air on the fracture wall can be neglected. The elastic modulus and Poisson's ratio of the mudstone samples remain unchanged due to the constant water content in the samples. Thus, the softening effect of the water should not be considered. For this part of the experiment, only the creep characteristics of the mudstone have an effect on the fracture opening.

The moisture content of the sample was increased to 7.0%. When the confining pressure is 1.0 MPa, the permeability coefficients of sample Y24 at the beginning and end of the experiment (after 60 hours) are both 1.30 × 10-7 m/s. Mudstone is still a low rheological rock under this condition. However, when the confining pressure increases to 2.5 MPa, the permeability of the mudstone sample Y26 exponentially decreases with time. When mudstone is saturated, its permeability coefficient decreases with time, regardless of the confining pressure (1.0 MPa or 2.5 MPa). When the confining pressure is 1.0 MPa, the permeability coefficient decreases more than 39%. When the confining pressure increases to 2.5 MPa, the permeability coefficient of Y25 decreases more than 79%.

As found in previous studies [28], rock viscoelasticity promotes fracture closure. When the specimen is saturated, the mudstone also exhibits viscous deformation at a lower confining pressure, and the viscous deformation of mudstone becomes more notable with the growth of confining pressure, and consequently, the closure of fractures becomes more pronounced. Therefore, the influence of the creep characteristics of mudstone on the fracture opening cannot be ignored.

Compared with the attenuation of the permeability coefficient of the specimen at the same confining pressure in Figure 9, which is 2~3 orders of magnitude, the attenuation in Figure 12 is less than an order of magnitude. In addition, water permeability experiments of saturated specimens with fractures also have been carried out at confining pressures of 1.0 MPa and 2.5 MPa. Because the permeability coefficient of the sample changes quickly, an accurate permeability is not obtained. The initial permeability coefficient of the specimens is less than 1.0 × 10-7 m/s, two orders of magnitude smaller than that in the previous experiment. It is highlighted again that the main reasons for fracture closure are both mudstone softening and viscoelastic behaviors.

Denudation has a minimal effect on the fracture closure, while mudstone softening and the creep of the mudstone itself cannot be disregarded. Mudstone softening and the viscosity of the mudstone reflect changes in the elastic modulus and Poisson's ratio of the mudstone matrix after water contact. Therefore, the self-closing capability of the mudstone fractures is the capability of the mudstone matrix to change its physical properties when the water content of the mudstone matrix increases. The capability of fracture self-closing can be estimated completely by use of the conventional mechanical and creep tests on mudstone samples.

6. Permeability Evolution of Fractured Mudstone Layers

In this section, we study the permeability evolution of fractured mudstone layer, which is one of overburdens over a coal seam including certain in-layer fractures due to native conditions or coal mining. At the engineering scale, the relationship between fracture hydraulic opening and the normal stress is usually obtained through experimental test fitting. The hyperbolic model currently widely used is:

$$b_{\mathrm{h}} = b_m - \frac{\sigma_n}{K_{n0} + \frac{\sigma_n}{b_m}} \tag{6}$$

where, b_h is hydraulic opening of fracture, b_m is initial hydraulic opening, σ_n is normal stress, and K_{n0} is initial normal stiffness of fracture. It is mentioned in Rutqvist's paper as an empirical expressions for the stress–fracture aperture relationship, and successfully to match laboratory measurements [29-30]. At the initial moment, the larger the contact area and the more dispersed the fracture, the greater the initial normal stiffness. When the initial contact area is constant, the initial normal stiffness, on the basis of the definition, is proportional to the elastic modulus of the mudstone matrix. Considering the self-closing factors of the mudstone fracture, the self-closing of the fracture is obviously because of the reduction of the normal stiffness of the fracture. Therefore, the normal stiffness of mudstone fractures can be expressed as a function of time. According to the testing of fractured mudstone with natural water content, the initial normal stiffness of the fracture is 1.08~1.57 $\times 10^{10}$ N/m^3, and the initial hydraulic opening is 2.19~3.00$\times 10^{-4}$ m. Additionally, there is little difference in such stiffnesses or openings for different mudstone fractures.

Based on the experimental data in section 4, the curve of the initial normal stiffness of the fracture K_{n0} with time can be obtained. Within minutes after the experiment started, the normal stiffness of the fractures rapidly decreased to 20~40% of the initial value. By the end of the experiment, about 72 hours, the initial normal stiffness of the fracture was 5.2~7.6$\times 10^8$ N/m^3, which was reduced to about 5% at the initial moment. Compared to the decrease of the elastic modulus of the mudstone, 1.3% of the initial value only, the initial normal stiffness of the fracture decreases relatively less, which is mainly due to the larger contact area at the end of the experiment. According to the analysis in the previous section, the opening of mudstone fractures does not change with time, so the initial normal stiffness of the fractures does not change with time.

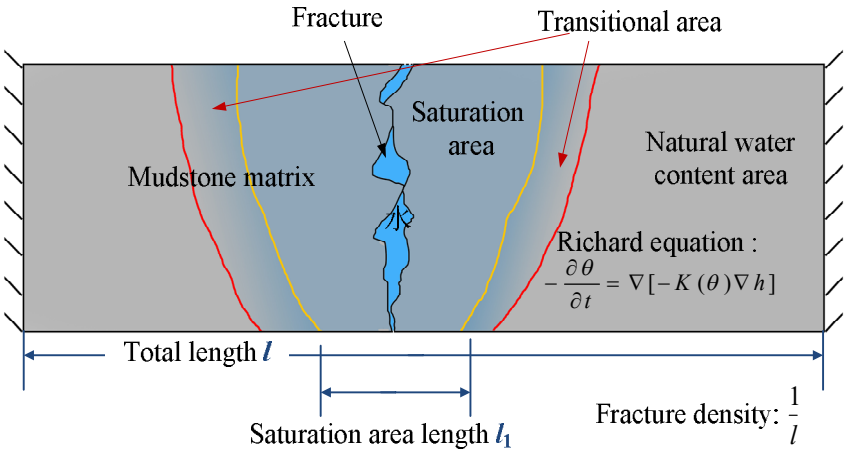

Figure 13. Schematic diagram of impermeability self-repairing of mudstone layer.

According to the experiments in section 4, the rock mass with the permeability coefficient less than 5.00 × 10-9 m/s is regarded impervious actually. If the permeability coefficient of the mudstone layer is less than 5.00 × 10-9 m/s, it is also correspondingly considered to have the capability to retain water. According to the mechanical properties of the material, the mudstone layer can be divided into three media: fractures, mudstone matrix with original water content, and mudstone matrix with saturated water content. It is assumed that all fractures in the mudstone layer are vertical and do not cross each other. The positional relationship between the three media is shown in Figure 13. The deformation of fractures mainly comes from the partial strain of

the mudstone matrix; the deformation of mudstone matrix mainly comes from the body strain of the mudstone matrix. It is also assumed that the water heads in the fractures are the same, so the thickness of water-saturated mudstone is the same. The deformation increment in the mudstone matrix along the fracture direction is 0, and the deformation increment mainly occurs in the normal direction of the fracture.

When the fracture density, a designing parameter in COMSOL, defined as the number of fractures per unit length of horizontal line, is constant; each unit boundary of the mudstone layer can be regarded as a fixed support, as shown in Figure 13, i.e. at any time, the displacement of the model boundary in the vertical direction of the fracture is 0 m.

$$\Delta s = s'_{\text{ini}} - s' = 0 \tag{7}$$

where, s'_{ini} is the displacement of the unit boundary in the vertical direction of the fracture at the initial moment and s' is the displacement at any moment.

When there is no water in the fracture, the deformation of the unit in the vertical direction of the fracture is only the change of the mechanical opening of the fracture and the displacement of the mudstone matrix with the original water content. The s'_{ini} value can be expressed as:

$$s'_{\text{ini}} = \Delta b_{\text{ini}} + \frac{\sigma_{\text{n0}} l}{E_{\text{ini}}} - \frac{\nu_{\text{ini}} \sigma_{\text{par1}} l}{E_{\text{ini}}} - \frac{\nu_{\text{ini}} \sigma_{\text{par2}} l}{E_{\text{ini}}} \tag{8}$$

where, Δb_{ini} is the change of the mechanical opening of the fracture at the initial moment. It is assumed that the average mechanical opening of the fracture is always equal to the hydraulic opening. σ_{n0} is the normal stress of fracture at initial moment, E_{ini} is the elastic modulus of mudstone matrix with natural moisture content, and σ_{par1} and σ_{par2} are the principal stresses parallel to the fracture direction at the initial moment.

When the fracture contains water, the water immerses into the mudstone matrix. The deformation of the unit in the vertical direction of the fracture includes the changes in the mechanical opening of the fracture, the deformation of mudstone matrix with original water content, and the deformation of water-saturated mudstone matrix. The displacement at this moment can be expressed as:

$$s' = \Delta b' + \frac{\sigma'_{\text{n}} l_1}{E_{\text{ini}}} - \frac{\nu_{\text{ini}} \sigma'_{\text{par1}} l_1}{E_{\text{ini}}} - \frac{\nu_{\text{ini}} \sigma'_{\text{par2}} l_1}{E_{\text{ini}}} + \frac{\sigma'_{\text{n}} l_2}{E_{\text{sat}}} - \frac{\nu_{\text{sat}} \sigma'_{\text{par3}} l_2}{E_{\text{sat}}} - \frac{\nu_{\text{satini}} \sigma'_{\text{par4}} l_2}{E_{\text{sat}}} - \frac{K_m l_2}{3} \tag{9}$$

where, $\Delta b'$ is the changes in the mechanical opening of the fracture at a certain time, σ'_{n} is the normal stress of the fracture at a certain time, E_{sat} is the elastic modulus of mudstone matrix with saturated water content, σ'_{par1} and σ'_{par2} are the principal stresses of natural mudstone matrix parallel to the fracture direction at a certain time, σ'_{par3} and σ'_{par4} are the corresponding principal stress of water-saturated mudstone matrix at a certain time, l_1 is the thickness of the original mudstone matrix in the vertical direction of the fracture at a certain time, and $l_2 = l - l_1$ is the thickness of the mudstone matrix with saturated water content in the vertical direction of the fracture.

The strain increase of the mudstone matrix in the direction of the fracture is 0, so the following relationship exists:

$$\Delta\sigma_{\text{par1}} = \Delta\sigma_{\text{par2}} = \frac{\nu_{\text{ini}} \Delta\sigma_{\text{n}}}{1 - \nu_{\text{ini}}} \tag{10}$$

$$\sigma_{\text{par3}} = \sigma_{\text{par4}} = \frac{3\nu_{\text{sat}} \sigma_{\text{n}} + \varepsilon_{\text{s}} E_{\text{sat}}}{3(1 - \nu_{\text{sat}})} \tag{11}$$

The fracture opening degree in any condition is obtained by the calculating formula (7) to (11). We use experimental data as the calculation parameters: the hydraulic head in the fracture is 10 m, the initial opening is 2.39×10^{-4} m; the initial normal stiffness of the fracture in the natural state is 1.38×10^{10} N/m^3; and the initial normal stiffness of the fracture is 6.2×10^{8} N/m^3 after the mudstone is saturated for 3 days. The calculation results and changes are shown in Figures 14~16.

For all fracture densities (0.01~10), the permeability coefficient of the mudstone layer far exceeds 5.00×10^{-9} m/s at the beginning when the fracture is formed. Over time, the initial normal stiffness of the fractures decreases and the volume

of saturated mudstones gradually increases (including softening and expansion strains), which reduces the hydraulic opening of the mudstone fractures. The permeability of the mudstone layer is less than 5.00×10^{-9} m/s after a period of time. This period of time is the repair time for the impermeable restoration of the mudstone layer. When the fracture density is constant, the repair time decreases as the horizontal in-situ stress increases, as shown in Figure 14. If the in-situ stress is large enough that the repair time of the mudstone layer is less than one day, we define the minimum in-situ stress as the lower limit of rapid repair stress. The curve of the lower limit of rapid repair stress is shown in Figure 15. The lower limit of rapid repair stress increases with the increase of fracture density.

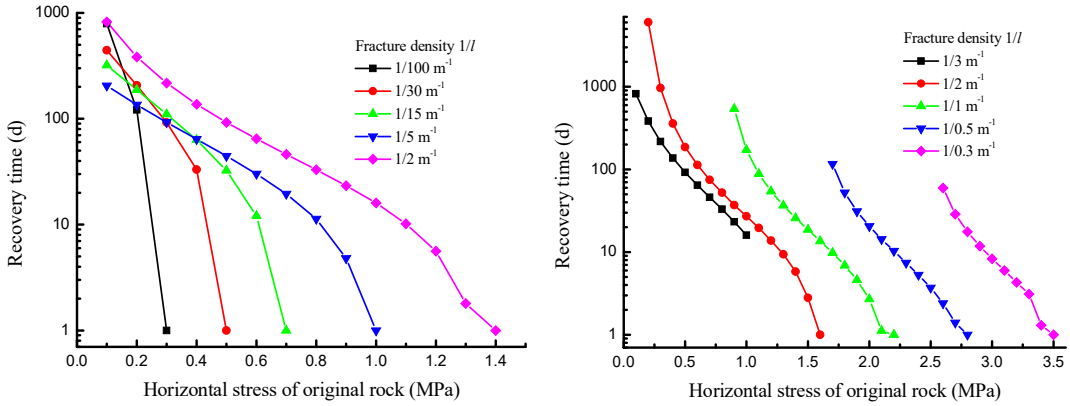

Figure 14. Repairing time of a fractured mudstone layer corresponding to different fracture densities.

When the fracture density is less than 0.33, i.e. $1/l \le 0.33$, the permeability of the mudstone layer will gradually return to the impermeable state under the action of minimal stress (0.3 MPa), and the fracture density 0.33 corresponds to the lower limit of rapid repair stress about 1.2MPa. When the fracture density is greater than 0.5, i.e. $1/l \ge 0.5$; all mudstone matrices are saturated with water in the fracture in a short period of time. The time to saturate all mudstone matrices can be the healing time limit of the mudstone layer. Furthermore, the healing limit decreases with the increase of fracture density, shown in Figure 16. When the fracture density is 10, the healing limit is about 23 days. If the in-situ stress is small, the impermeability of the mudstone layer cannot totally recover within the time limit, and also it cannot go on completing recovery even if the time limit is exceeded. Therefore, ensuring sufficient in-situ stress is a necessary condition for impermeable restorations of mudstone layers. The minimum in-situ stress for repairing impermeability of mudstone layers is the lower limit of recovery stress. This lower limit increases with the increase of fracture density, and its change curve is also shown in Figure 16.

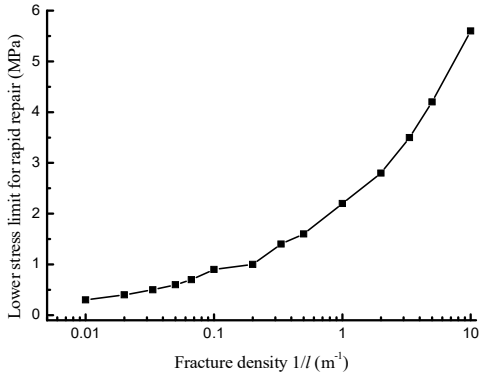

Figure 15. The lower limits of rapid repair stress of a fractured mudstone layer corresponding to different fracture densities

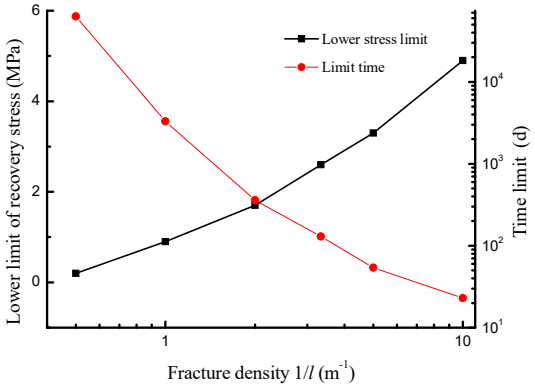

Figure 16. The time limits and lower limits of stress for impermeability recovery of mudstone layers.

In summary, smaller fracture density and greater in-situ stress are advantageous to the impermeable restoration of mudstone layers. When the fracture density is small and the in-situ stress is large, the mudstone layer has no self-repairing capability. At this time, external intervention is required to make the mudstone layer have water-proof capability. The main means of external intervention can start from the application of increasing the nearby stress or reducing the fractures density.

At the same time, the volume of the saturated mudstone matrix increased with the increase of the water head in the fracture. With the same fracture density and in-situ stress, increasing the hydraulic head in the fracture to 30 m, the impervious recovery speed can be faster and the time limit is smaller. The calculation shows that, however, its effect on the lower limit of the recovery stress and the lower limit of the rapid repair stress becomes not obvious. Therefore, the variation of water head in a slight crack has little effect on the impermeable recovery of mudstone.

In the actual working conditions of Yili No. 4 Mine, the mudstones in the third and sixth layers are the main impermeable layers. The horizontal stress of shallow rock layer in Yili area has a linear relationship with the depth. It can be easily estimated that the horizontal stress of the third layer of mudstone is between 1.0~9.7 MPa, and the horizontal stress of the sixth layer of mudstone is between 1.8~13.2 MPa. According to the previous calculations, the fracture density is determined to make the mudstone layer impermeable. The fracture density of the third mudstone layer can be repaired when the density is less than 1.1, and can be repaired quickly when it is less than 0.2. The longest repair time is around 120 days. The fracture density of the sixth mudstone layer can be repaired when the density is less than 2.2, and can be repaired quickly when it is less than 0.6. The longest repair time is around 50 days. When one of the two mudstone layers is impermeable, soil water will not be lost.

At present, the Yili No. 4 Mine uses a rapid-propulsion mining method, and the density of fractures in the corresponding rock layer above the coal seam is less than 1. The condition that the impermeability of mudstone layers cannot be repaired is that the density of fractures in the third layer, where one of the corresponding layers is located, is greater than 1.1, and the density of fractures in the sixth layer, where the other corresponding layer is located, is greater than 2.2. Thereby, we judge that soil water will not be lost along fractures in such layers. The surface of the mining area is the summer pasture of the local herdsmen. The ground after mining is leveled in winter and can still be grazed the following summer. This phenomenon proves that there is no loss of soil water, consistent with previous judgments.

When the conditions of the mudstone are suitable, the mudstone layer will always have lower permeability. This study could improve future seepage analyses of underground rock masses, also serving as references for seismic hydrological evolution and nuclear waste storage.

7. Conclusions

In this paper, the mechanical properties of mudstone with different water contents are investigated by performing experiments and analyzing the experiment results. A seepage test system considering fracture closure is designed and built. With the system, the behavior and mechanism of mudstone fracture closure are examined on the basis of its outcomes. Also based on experimental data, the tendency of permeability attenuation of the fractured mudstone layer was calculated with the COMSOL platform, and the soil water change after mining was furthermore analyzed. The main conclusions are as follows.

1) As the water content and normal stress of the mudstone increase, its viscoelasticity becomes more pronounced, and the permeability coefficient of the single-fracture mudstone samples exhibits more significant exponential attenuation. In water seepage experiments with single-fracture mudstone samples at natural water content, the permeability coefficient decreases exponentially over time, even with a reduction of more than two orders of magnitude. When the normal stress on the fracture exceeds 2.0~2.5 MPa, the mudstone fracture will close rapidly and completely (with a hydraulic opening smaller than 6.27×10^{-6} m) as time progresses.

2) The factors influencing mudstone fracture self-closing are summarized as follows: water-induced denudation of the fracture walls, mudstone softening due to water, and mudstone creep after water exposure. In the complete process of fracture closure, mudstone softening plays a dominant and fundamental role, while the creep behavior of the mudstone is also significant, but water-induced denudation has only a minimal impact. In effect, mudstone softening and creep behavior reflect the variations of elastic modulus and Poisson's ratio of the mudstone matrix under the water-soaked condition. Thus, the self-closing capacity of the fractures can be evaluated completely by use of

conventional mechanical and creep tests on mudstone samples.

3) At the engineering scale, the key factor for fracture self-closing is either the in-situ stress around fractures or the density of in-layer fractures. If the in-situ stress is larger than the minimum repairing limit, the recovery behavior of the mudstone layer can always be completed and the larger compression contributes the quicker recovery. In addition, a lower fracture density can also favor the impermeable restoration of mudstone layers, and the critical fracture density depends on the minimum repairing stress. Consistently, both the calculating analysis and field observations demonstrate that the overlying mudstone layers in Yili No.4 mine can regain its impermeability within a certain period after mining.

Declaration of Competing Interest

We, the undersigned corresponding author, also certify that I/we have no commercial associations (e.g., consultancies, stock ownership, equity interests, patent-licensing arrangements, etc.) that might pose a conflict of interest in connection with the submitted article, except as disclosed on a separate attachment. All funding sources supporting the work and all institutional or corporate affiliations of mine/ours are acknowledged in a footnote.

Acknowledgments

This study was supported by a Special Subject Grant of the National "973" Basic Research Program of China (No. 2015CB251602), National Major Project of Science and Technology (2016ZX05043), Jiangsu Natural Science Foundation (BK20180636), Independent Innovation Project for Double First-level Construction of CUMT (2018ZZCX04), National Natural Science Foundation of China (No.12202483), Special Scientific Research Project of Innovation and Entrepreneurship of China Coal Research Institute (2021-KXYJ-007), and Special Project of Science and Technology Innovation and Entrepreneurship Fund of Tiandi Science and Technology Co. Ltd. Technology R&D and Application (2023-TD-ZD004-004). Special thanks to the anonymous reviewers for their invaluable comments.

Data Availability Statement

All data, models, and code generated or used during the study appear in the submitted article.

References

[1]. Davy, C. A., Skoczylas, F., Barnichon, J. D., & Lebon, P. (2007). Permeability of macro-cracked argillite under confinement: Gas and water testing. *Physics and Chemistry of the Earth, Parts A/B/C, 32*(8–14), 667–680.

[2]. Van Marcke, P., & Bastiaens, W. (2010). Excavation induced fractures in a plastic clay formation: Observations at the Hades URF. *Journal of Structural Geology, 32*(11), 1677–1684.

[3]. Qin, H., Tang, H., Yin, X., Cheng, X., & Li, J. (2024). Study on water–rock interaction failure mechanism and constitutive model of mudstone damaged by pre-peak disturbance. *Theoretical and Applied Fracture Mechanics, 133*, 104539.

[4]. Pan, D., Liu, C., Liang, D., Zhou, J., & Zhang, L. (2024). Study on time-dependent injectability evaluation of mudstone considering the self-healing effect. *Open Geosciences, 16*, 16–27.

[5]. Zhang, D., Fan, G., Ma, L., & Wang, X. (2011). Aquifer protection during longwall mining of shallow coal seams: A case study in the Shendong coalfield of China. *International Journal of Coal Geology, 86*(2), 190–196.

[6]. Li, X., Li, X., Wang, Y., Peng, W., Fan, X., Cao, Z., & Liu, R. (2023). The seepage evolution mechanism of variable mass of broken rock in karst collapse column under the influence of mining stress. *Geofluids*, 1–10.

[7]. Zhang, C. (2011). Experimental evidence for self-sealing of fractures in claystone. *Physics and Chemistry of the Earth, Parts A/B/C, 36*(17–18), 1972–1980.

[8]. Abdollahipour, A., Marji, M. F., Bafghi, A. Y., & Gholamnejad, J. (2016). Numerical investigation of effect of crack geometrical parameters on hydraulic fracturing process of hydrocarbon reservoirs. *Journal of Mining and Environment, 7*(2), 205–214.

[9]. Abdollahipour, A., Marji, M. F., Bafghi, A. Y., & Gholamnejad, J. (2016). A complete formulation of an indirect boundary element method for poroelastic rocks. *Computers and Geotechnics, 74*, 15–25.

[10]. Ma, T., Rutqvist, J., Oldenburg, C. M., & Liu, W. (2017). Coupled thermal–hydrological–mechanical modeling of CO2-enhanced coalbed methane recovery. *International Journal of Coal Geology, 179*, 81–91.

[11]. Baghbanan, A., & Jing, L. (2008). Stress effects on permeability in a fractured rock mass with correlated fracture length and aperture. *International Journal of Rock Mechanics and Mining Sciences, 45*(8), 1320–1334.

[12]. Bastiaens, W., Bernier, F., & Li, X. L. (2007). Selfrac: Experiments and conclusions on fracturing, self-healing and self-sealing processes in clays. *Physics and Chemistry of the Earth, Parts A/B/C, 32*(8–14), 600–615.

[13]. Wang, L. L., Bornert, M., Héripré, E., Chanchole, S., Pouya, A., & Halphen, B. (2015). The mechanisms of deformation and damage of mudstones: A micro-scale study combining ESEM and DIC. *Rock Mechanics and Rock Engineering, 48*(5), 1913–1926.

[14]. Nahazanan, H., Clarke, S., Asadi, A., Md. Yusoff, Z., & Kim Huat, B. (2013). Effect of inundation on shear strength characteristics of mudstone backfill. *Engineering Geology, 158*, 48–56.

[15]. Fukuda, D., Maruyama, M., Nara, Y., Hayashi, D., Ogawa, H., & Kaneko, K. (2014). Observation of fracture sealing in high-strength and ultra-low-permeability concrete by micro-focus X-ray CT and SEM/EDX. *International Journal of Fracture, 188*(2), 159–171.

[16]. Cao, P., Karpyn, Z. T., & Li, L. (2015). Self-healing of cement fractures under dynamic flow of CO2-rich brine. *Water Resources Research, 51*(6), 4684–4701.

[17]. Polak, A., Elsworth, D., Yasuhara, H., Grader, A. S., & Halleck, P. M. (2003). Permeability reduction of a natural fracture under net dissolution by hydrothermal fluids. *Geophysical Research Letters, 30*(20).

[18]. Hearn, N., & Morley, C. T. (1997). Self-sealing property of concrete—Experimental evidence. *Materials & Structures, 30*(7), 404–411.

[19]. Brunet, J. L., Li, L., Karpyn, Z. T., & Huerta, N. J. (2016). Fracture opening or self-sealing: Critical residence time as a unifying parameter for cement–CO2–brine interactions. International Journal of Greenhouse Gas Control, 47, 25–37.

[20]. Hou, Z. (2003). Mechanical and hydraulic behavior of rock salt in the excavation disturbed zone around underground facilities. *International Journal of Rock Mechanics and Mining Sciences, 40*(5), 725–738.

[21]. Zhong, Y., Kuru, E., Zhang, H., Kuang, J., & She, J. (2019). Effect of fracturing fluid/shale rock interaction on the rock physical and mechanical properties, the proppant embedment depth and the fracture conductivity. *Rock Mechanics and Rock Engineering, 52*(4), 1011–1022.

[22]. Vahab, M., & Khalili, N. (2018). X-FEM modeling of multizone hydraulic fracturing treatments within saturated porous media. *Rock Mechanics and Rock Engineering, 51*(10), 3219–3239.

[23]. Malama, B., & Kulatilake, P. H. S. W. (2003). Models for normal fracture deformation under compressive loading. *International Journal of Rock Mechanics and Mining Sciences, 40*(6), 893–901.

[24]. Misra, A., & Marangos, O. (2011). Rock-joint micromechanics: Relationship of roughness to closure and wave propagation. *International Journal of Geomechanics, 11*(6), 431–439.

[25]. Hopkins, D. L. (2000). The implications of joint deformation in analyzing the properties and behavior of fractured rock masses, underground excavations, and faults. *International Journal of Rock Mechanics and Mining Sciences, 37*(1), 175–202.

[26]. Sevostianov, I., & Kachanov, M. (2008). Normal and tangential compliances of interface of rough surfaces with contacts of elliptic shape. *International Journal of Solids and Structures, 45*(9), 2723–2736.

[27]. Marache, A., Riss, J., & Gentier, S. (2008). Experimental and modelled mechanical behaviour of a rock fracture under normal stress. *Rock Mechanics and Rock Engineering, 41*(6), 869–892.

[28]. Matsuki, K., Wang, E. Q., Sakaguchi, K., & Okumura, K. (2001). Time-dependent closure of a fracture with rough surfaces under constant normal stress. *International Journal of Rock Mechanics and Mining Sciences, 38*(5), 607–619.

[29]. Rutqvist, J., Wu, Y. S., Tsang, C. F., & Bodvarsson, G. (2002). A modeling approach for analysis of coupled multiphase fluid flow, heat transfer, and deformation in fractured porous rock. *International Journal of Rock Mechanics and Mining Sciences, 39*(4), 429–442.

[30]. Daley, T. M., Schoenberg, M. A., Rutqvist, J., & Nihei, K. T. (2006). Fractured reservoirs: An analysis of coupled elastodynamic and permeability changes from pore-pressure variation. *Geophysics, 71*(5), 33–41.

بررسی تجربی مکانیسم خود بسته شدن شکستگی‌های گل سنگی و تغییرات نفوذپذیری روباره معدن

ویکون لیو، تیان فانگ*، و شنگ سانگ

آزمایشگاه کلید دولتی برای ژئومکانیک و مهندسی زیرزمینی عمیق، دانشگاه معدن و فناوری چین، شو ژو ۲۲۱۱۱۶، جیانگ سو

ارسال ۲۰۲۴/۱۱/۰۳، پذیرش ۲۰۲۵/۰۱/۱۴

* نویسنده مسئول مکاتبات: 357421666@qq.com

چکیده:

گلسنگ سنگی رایج در مهندسی زیرزمینی است و گلسنگ با شکستگی قابلیت خود بسته شدن خاصی دارد. در این مقاله، ما از آزمایش‌ها و آنالیزهای عددی برای بررسی مکانیسم چنین مشخصه‌ای استفاده کردیم و همچنین الگوی نفوذپذیری بارهای مادستون را بررسی کردیم. آزمایش‌ها با سیستم آزمایش MTS815.02 انجام شد که شامل خواص مواد تحت محتویات مختلف آب و رفتارهای ترک ترک آنها می‌شد. وظیفه اصلی آنالیز عددی تعیین نفوذپذیری لایه‌های گل سنگ شکسته، کار با پلت فرم COMSOL است. نتایج تجربی نشان می‌دهد که مدول یانگ گل‌سنگ اشباع از آب فقط ۲/۲ درصد از گل‌سنگ طبیعی است، و اشباع‌شده نیز رفتار خزشی قابل‌توجهی از خود نشان می‌دهند. با افزایش فشارهای اطراف، ضریب نفوذپذیری گل سنگ شکسته به طور تصاعدی کاهش می‌یابد، حتی دو مرتبه قدر مربوط به فشارهای بیش از ۰.۲ MPa کاهش می‌یابد. بر اساس این نتایج آزمایش، به راحتی می‌توان استنباط کرد که شکستگی سریع یا کامل دلیل اصلی افت نفوذپذیری است، و علاوه بر این، نرم شدن و خزش عوامل اصلی خود بسته شدن شکستگی‌های گل سنگی هستند و به ویژه، رفتار نرم شدن نقش کاملاً اساسی ایفا می‌کند. تحلیل‌های عددی نشان می‌دهند که تنش درجا بالاتر یا چگالی شکست کمتر می‌تواند بدیهی باشد که یکی از شرایط سودمند برای لایه‌های گل سنگ شکسته برای بازگرداندن به سمت نفوذناپذیری باشد. این نتایج همچنین توسط مشاهدات مهندسی در معدن Yili شماره ۴ چین تأیید شده است. بدیهی است که پس از مدتی ظرفیت مسدود کردن آب اقشار پوشاننده بازیابی شده است. بدینوسیله ما این تحقیق را به عنوان مرجعی برای معدنکاری زیرزمینی یا ساخت و ساز مهندسی شامل گلسنگ توصیه می‌کنیم.

کلمات کلیدی: بسته شدن شکستگی، گل سنگ، رفتار نرم کننده کرنش، آب خاک، ترمیم غیر قابل نفوذ گلسنگ.